Journal of Manufacturing Engineering, March, 2012, Vol. 7, Issue. 1, pp 16 - 22

ANALYSIS OF COMPOSITE ROTATING DISCS

*** Ramesh N**[1], **Raghu Kumar B**[2] **and Durga Prasad G**[3]

[1, 2, 3] Department of Mechanical Engineering, K L University, Vijayawada, Andhra Pradesh-520002, India

ABSTRACT

The effects of centrifugal forces on stresses and deformations are important for the design of rotating discs. The disc is made out of composite laminate plate which is considered to be specially orthotropic. Different composite materials with different laminate sequences have been used for investigating the radial and tangential stress resultants in addition to displacements. Classical laminate plate theory is used in the analysis to study the effect of anisotropy on the rotating disc stress distribution. Stresses and displacements are also found from the Finite Element Software. .A stiffness ratio is defined as the ratio of circumferential stiffness to radial stiffness and this is used as a parameter to represent the degree of anisotropy. Results obtained from this investigation for stresses and displacements have been tabulated and presented graphically. These results are useful for the design of rotating discs.

Key words: *Composite Material, Rotating Disc and Fiber Reinforcement*

1. Introduction

Rotating disc is a very useful component in many engineering applications. Such as turbines, rotors, compressors, flywheels and computer's disc drive. Many of these applications require Effect of centrifugal forces on stresses and displacements great deal of work has been dedicated to area of Effect of centrifugal forces on stresses and displacements have been studied for different composite laminated rotating discs.

Many papers appeared in the analysis of laminated rotating disc. With increasing demand for higher strength to weight ratios, optimizing the geometrical and physical properties of disc configuration becomes more significant. Seireg and surana [1] presented a numerical technique to obtain optimum configuration in isotropic rotating discs.

Anisotropy was investigated by Murthy and Sherbourne [2] and Reddy and Srinath [3] handled variable density and variable thickness in rotating discs. Chang [4], Gurushankar [5], Christensen and Wu [6] and Genta and Gola [7] dealt with determining stresses via an elasticity approach in orthotropic single- ply circular plates with the outer boundary free of any constraints. Bert [8] used a laminated plate theory on layered plates with extension–bending coupling, and with stress free boundaries by which approximate solutions were obtained.

The displacement equation of a rotating isotropic circular plate was given in a paper by Mostaghel and Tadjbakhsh [9] as they attempted to examine the stability of rotating isotropic rods and plates when the boundary was restrained to prevent motion. The analytical solution of elastic perfectly plastic rotating discs of constant thickness and density was studied by Gamer [10] using Tresca's condition.

Gamer [11, 12] also studied the analytical solutions of such disks with a linear strain-hardening material behavior using the same yield condition. Guven [13] extended this work to rotating disks of thickness function $h= h_o (r/b)^{-n}$ and density function $\rho =\rho_o(r/b)^m$ and obtained their analytical solution using the same material behavior and yield condition.

Sterner et al. [14] pointed that, the numerical analysis usually require extensive computer resources, are tedious to perform due to extensive meshing requirements and are expensive, making them unsuitable for the elastic analysis of rotating disk with a general, arbitrary configuration based on the repeated application of a truncated Taylor's expansion. NakiTutuneu [15] determined stresses and deformation resulting from centrifugal forces in rotating specially orthotropic plates.

The classical laminate plate theory is employed in the analysis and the results are presented in a manner which illustrates the effect of anisotropy. The plate is assumed to be rigidly fixed to a concentric rod allowing no deformation in its central region. The outer boundary is either free of any constraints or the plate is placed in a stiff casing which presents radial deformation. Jen-san Chen and jhi-Lu jhu [16] investigated the in plane response of a rotating annular disk under concentrated edge loads with both the radial and tangential components.

**Corresponding Author - E- mail: ramesh_65nutakki@yahoo.co.in*

Lames's potentials are used to simplify the highly coupled equilibrium equations. It is demonstrated that the problem of fixed disk-rotating load differs from the problem of rotating disk fixed load not only by the centrifugal effect, but also by additional terms arising from Coriolis Effect. While the effect of these coriokis terms may be negligible when rotational speed is small or the concentrated edge load is in radial direction, they are important in the high rotational speed range when the concentrated edge load is in the tangential direction. Rajeev jain et al. [17] proposed a procedure to design a constant thickness composite disk of uniform strength by radially tailoring the anisotropic elastic constants. A special case of an isotropic disc with radially varying modulus is also examined. Analytical results were also compared with FEM calculations for two cases of radially varying anisotropy and for an isotropic disk with variable modulus.

Lou at al. [18] developed a numerical method for the analysis of deformations and stresses in elastic-plastic rotating disks with arbitrary cross section of continuously variable thickness and arbitrarily variable density made of non-linear strain hardening materials. In the present study, the effect of laminated orthotropic circular plates used for rotating discs on the stress distribution has been analyzed. Two boundary conditions are considered:

(i) Constraint free outer boundary and

(ii) Fixed outer boundary.

Further different composite materials have been chosen for the analysis to highlight the effect on the stress distribution.

2. Stress-Strain Relations

A circular plate of radius R and having uniform thickness is rotating at angular velocity ω. Assuming steady rotation symmetric deformation with no bending, displacements are described as:

Displacement in radial direction r, u = f(r)

Displacement in tangential direction θ, v = 0

Displacement in axial direction, w = 0 (**1**)

For an axi-symmetric problem, stresses and strains are independent of tangential coordinate θ. The in-plane strain components are

$$\varepsilon_r = \frac{du}{dr}, \varepsilon_\theta = \frac{u}{r} and \gamma_{r\theta} = 0 \qquad (2)$$

For specially orthotropic and symmetric circular laminated plates, there is no coupling between in plane and bending equations. The stress strain relations are

$$\begin{bmatrix} N_r \\ N_\theta \\ N_{r\theta} \end{bmatrix} = \begin{bmatrix} A_{11} & A_{12} & 0 \\ A_{21} & A_{22} & 0 \\ 0 & 0 & A_{66} \end{bmatrix} \begin{bmatrix} \varepsilon_r \\ \varepsilon_\theta \\ 0 \end{bmatrix} \qquad (3)$$

WhereN_r, N_θ are stresses per unit length in the radial and tangential directions and terms A_{ij} are defined as,

$$A_{ij} = \sum_{k=0}^{n} \overline{Q}_{ij} (Z_K - Z_{K-1}) \qquad (4)$$

Where n is the total number of plies in the laminate, k is the ply number starting from the midplane as shown in fig. 1 and Z_k, Z_{k-1} are distances bottom and top of the K^{th} ply from the midplane of the laminate ($Z = 0$).

The transformed in-plane stiffness matrix of the K^{th} ply $\bar{Q}_{ij}^{(k)}$ are given by equation $\overline{Q} = [T]_\sigma [Q][T]_\varepsilon$

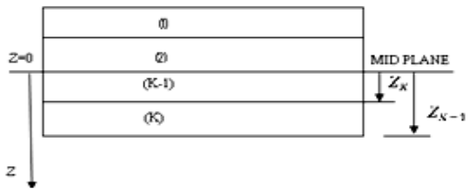

Fig. 1 Ply Distance

Substituting equation (2) into (3),

$$N_r = A_{11}\varepsilon_r + A_{12}\varepsilon_\theta = A_{11}\frac{du}{dr} + A_{12}\frac{u}{r} \qquad (5)$$

$$N_\theta = A_{21}\varepsilon_r + A_{22}\varepsilon_\theta = A_{21}\frac{du}{dr} + A_{22}\frac{u}{r} \qquad (6)$$

3. Equilibrium Equation

The governing differential equation in the radial direction is,

$$\frac{1}{r}\frac{d}{dr}[(rN_r) - N_\theta] + \rho\omega^2 r = 0 \qquad (7)$$

Where 'ρ' is the mass per unit area. The applied force on the disk per unit area is the centrifugal force. Substitution of expression for N_r and N_θ from equations (5) and (6) into equation (7)

$$r^2u'' + ru' - \frac{A_{22}}{A_{11}}u + \frac{\rho\omega^2 r^3}{A} = 0 \qquad (8)$$

Where primes denote differentiation with respect to r. Solution for the above equation is,

$$u = C_1 r^\lambda + C_2 r^{-\lambda} + \frac{\rho\omega^2}{A_{11}(\lambda^2 - 9)} r^3 \qquad (9)$$

$$where\ \lambda = \sqrt{\frac{A_{22}}{A_{11}}}$$

When $\lambda^2 = 9$, the expression for radial displacement,

$$u = D_1 r^3 + D_3 r^{-3} + \left(\frac{1 - 6\log r}{36A_{11}}\right)\rho\omega^2 r^3 \qquad (10)$$

The constants are evaluated using boundary conditions.

4. Boundary Conditions

Two different boundary conditions are considered.

1. The disk is not constrained at the boundary
2. The disk is constrained at the boundary

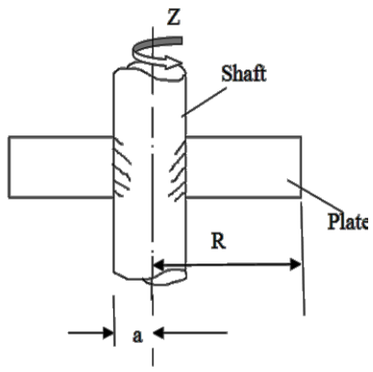

Fig. 2 Configuration of Rotating Disk

4.1 Constraint free boundary

The inner radius of the disk is 'a' and fixed on the shaft rotating at an angular velocity 'ω' about Z-axis as shown in configuration diagram fig. 2. The constants of integration$C_1$and C_2 in Eq. (3.9) are evaluated using the boundary conditions:

i) at $r = a$, the radial displacements $u = 0$

ii) at $r = a$, the radial stress $N_r = 0$

The constants of the integration C_1 and C_2 are given by the expressions.

$$C_1 = \frac{\rho\omega^2\left[R^{l_4} + a^{l_4}F_3\right]}{F_4} \quad (11)$$

$$C_2 = \frac{\rho\omega^2\left[(Ra)^{l_1}R^{l_1}F_1 - R^3a^{l_1}F_2\right]}{F_4} \quad (12)$$

$$l_1 = \lambda, \quad l_2 = \lambda - 1, \quad l_3 = \lambda + 1, \quad l_4 = \lambda + 3,$$
$$l_5 = 2\lambda, \; l_6 = \lambda^2, \; l_7 = \left(9 - \lambda^2\right)$$
$$b_1 = A_{11}, \; b_2 = A_{12}, \; a = 0.05m,$$
$$R = 0.5M$$
$$F_1 = (\lambda A_{11} + A_{12}) = (l_1 b_1 + b_2)$$
$$F_2 = (3A_{11} + A_{12}) = (3b_1 + b_2)$$
$$F_4 = b_1 l_9\left[R^{l_5}F_1 + a^{l_5}F_2\right] \quad (13)$$

Stress N_r and N_θ are obtained using the radial displacements obtained from equation (3) with the following relations.

$$N_r = A_{11}\frac{du}{dr} + A_{12}\frac{U}{R} \quad (14)$$

$$N_\theta = A_{12}\frac{du}{dr} + A_{22}\frac{U}{R} \quad (15)$$

$$\frac{N_r}{\rho\omega^2} = G_1 r^{l_2}F_2 - G_2 r^{-l_3} - \frac{r^2F_2}{b_1 l_9} \quad (16)$$

$$G_1 = \frac{\left(R^{l_4}F_2 + a^{l_4}F_3\right)}{F_4} \quad (17)$$

$$G_2 = \frac{(Ra)^{l_1}\left[R^{l_1}a^3F_1 - R^3a^{l_1}F_2\right]}{F_4} \quad (18)$$

$$\frac{N_\theta}{\rho\omega^2} = G_1 r^{l_2}F_5 - G_2 r^{-l_3}F_6 - \frac{A_{21}3r^2}{A_{11}^{l_7}} - \frac{r^3}{l_7} \quad (19)$$

$$F_5 = (\lambda A_{21} + A_{22}), F_6 = (\lambda A_{21} - A_{22}),$$
$$U = G_1 r^{\lambda} + G_2 r^{-\lambda} + \frac{r^3}{b_1(-l_7)} \quad (20)$$

Fixed boundary condition

$$C_1 = \frac{\rho\omega^2(R^\alpha - A^\alpha)}{F_5} \quad (21)$$

$$C_2 = \frac{\rho\omega^2 R^\lambda a^\lambda \varepsilon}{F_5} \quad (22)$$

$$b_1 = \lambda - 1, b_2 = \lambda + 1, P = \left(9 - \lambda^2\right), \alpha = 3 + \lambda = \left(R^{2\lambda} - a^{2\lambda}\right), \varepsilon = \left(R^\lambda a^3 - R^3 a^\lambda\right)$$
$$F_1 = (\lambda A_{11} + A_{12}), F_2 = (\lambda A_{11} - A_{12}), \; F_3 = \frac{3r^2}{P}, F_4 = \frac{A_{21}r^2}{A_{11}P}, F_5 = A_{11}\rho\beta \quad (23)$$

Stress N_r and N_θ are obtained using the radial displacements obtained from equation (9) using fallowing relations (14) and (15).

$$\frac{N_r}{\rho\omega^2} = D_1 r^{b_1}F_1 - D_2 r^{-b_2}F_2 - F_3 - F_4 \quad (24)$$

$$D_1 = \frac{(R^\alpha - a^\alpha)}{F_5} \quad (25)$$

$$D_2 = \frac{R^\lambda a^\lambda \varepsilon}{F_5} \quad (26)$$

$$\frac{N_\theta}{\rho\omega^2} = D_1 r^{b_1}F_1 - D_2 r^{-b_2}F_2 - F_6 - F_7 \quad (27)$$

$$F_6 = \frac{A_{21}3r^2}{A_{11}P}, F_7 = \frac{r^2}{P}$$
$$U = D_1 r^{\lambda} + D_2 r^{-\lambda} + \frac{r^3}{A_{11}(-P)} \quad (28)$$

5. Results and Discussions

Stresses and displacements have been calculated using above equations for constraint free and fixed boundary conditions. These values are also calculated using ANSYS. Fig. 3 shows the mesh pattern of a rotating disc. The shell linear layered 99 element has been used. Fig. 4 and fig. 5 shows the stress and displacement patterns for rotating disc.

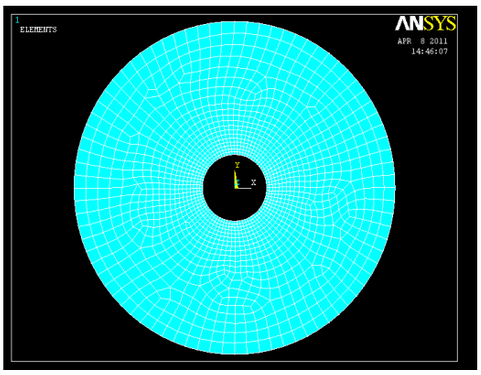

Fig.3 Meshed Model

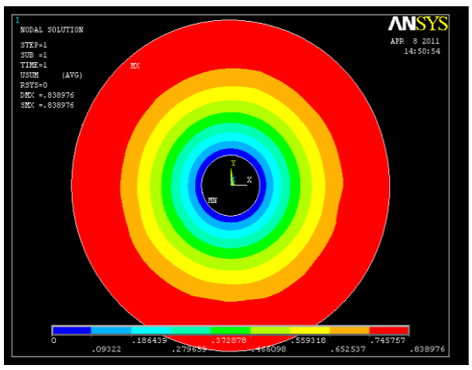

Fig. 4 Plot for U_{sum} Radial Displacements

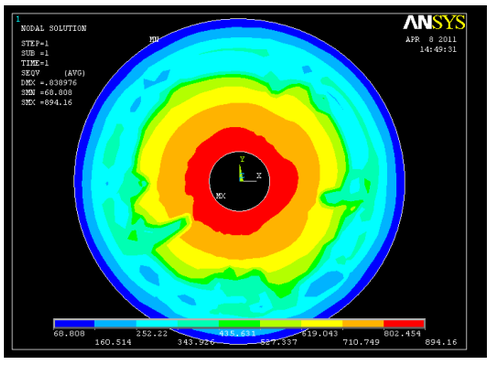

Fig. 5 Plot for Radial Stress

Five composite materials have been chosen for analysis such as (1) Graphite/Epoxy (2) Kevlar/Epoxy (3) Boron/Epoxy (4) Boron/Aluminum, and (5) Scs-6/Ti-15-3. The properties of material are shown in table 1.

Table: 1 Property of Composite Materials

Composite Materials	E_1 (GPa)	E_2 (GPa)	G_{12} (GPa)	υ_{12}	v_f
Graphite/Epoxy	138	9	6.9	0.5	0.25
Kevlar/Epoxy	75.8	5.5	2.3	0.34	0.65
Boron/ Epoxy	204	18.5	5.59	0.23	0.5
Boron/Al	227	139	57.6	0.24	0.46
SCS-6/Ti-15-3	221	145	53.2	0.27	0.39

E_1 is longitudinal modulus of composite
E_2 is transverse modulus of composite
G_{12} is in-plane shear modulus of composite
υ_{12} is major poisson's ratio
V_f is volume fraction of fiber

Two symmetric laminates are considered for the evaluation of stresses and displacements.

i) $[45/-45/-45/45]$ laminates made out of four composite materials and $\lambda^2 = 1$
ii) $[0/90/90/0]$ laminates with equal number of 0^0 and 90^0 fiber angle lamina and $\lambda^2 = 1$
iii) Laminates with different number of layers 0^0 and 90^0 so that the effect of stiffness ratio can be studied with various values of λ^2.

Radial stresses have been graphically represented for $[45/-45]_s$laminate with respect to variation in radius for constraint free boundary condition in Fig. 6 for constraint free boundary condition, the radial stresses are zero at the outer radius of disc. Radial stresses increases towards the inner radius. Maximum radial stress is observed in case of Scs- 6/ Ti-15-3 composite material and minimum in case of Kevlar/ epoxy material at $r = 0.05m$. At $r = 0.2m$ Kevlar/ Epoxy shows higher values of radius stresses than other composite and beyond $r = 0.2m$ studiedly decreases to zero at $r = 0.5m$.

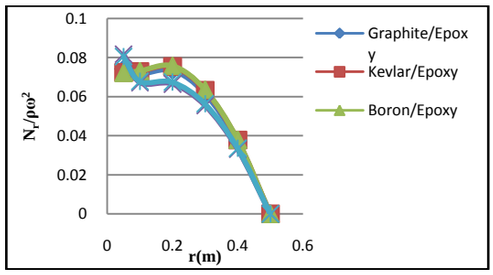

Fig. 6 Radial Stresses for Constraint Free Boundary Condition $[45/-45/-45/45]$

For fixed boundary conditions the radial stress is tensile and changes to compressive stress in between $r = 0.3m$ and $r = 0.4m$ as shown in figure 7.

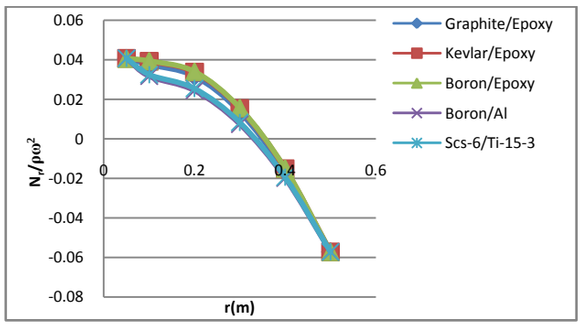

Fig. 7 Radial Stresses for Fixed Boundary Condition $[45/-45/-45/45]$

Fig.8 shows the radial displacements as a function of radial distance for constraint free boundary condition. Radial displacement for Kevlar/Epoxy is larger than other composites and lowest displacement is displayed by graphite/epoxy composite.

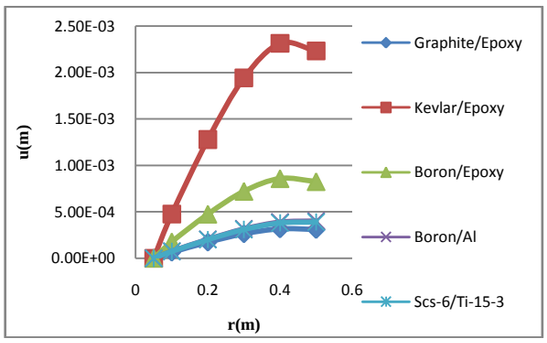

Fig. 8 Radial Displacements for Constraint Free Boundary Condition $[45/-45/-45/45]$

Graphical representations of radial displacements as a function of radius are represented in Fig. 9 for fixed boundary condition. Radial displacements vary from zero at $r = 0.5$m to maximum at $r = 0.3$m and finally reaching zero at $r = 0.5$m for all composites. The variation of displacements is maximum for Kevlar/Epoxy and lower for Graphite/Epoxy and very close to Scs- 6/ Ti-15-3. The displacements are higher in constraint free boundary than in fixed boundary.

Cross ply symmetric laminates having layers of $[0/90]_s$ are considered for analyzing stress distribution and displacements using different materials for composites. Radial stress distribution as a function of

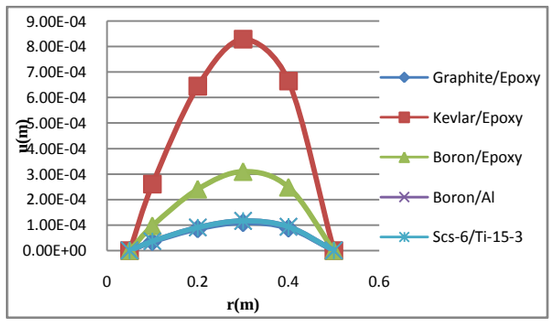

Fig. 9 Radial Displacements Fixed boundary condition $[45/-45/-45/45]$

radius is graphically represented in figure 10 for constraint free boundary In constraint free boundary condition, the radial stresses different materials are nearly equal showing maximum at r = 0.05m and zero at r = 0.5m. The trend is depicted as shown in figure 10.

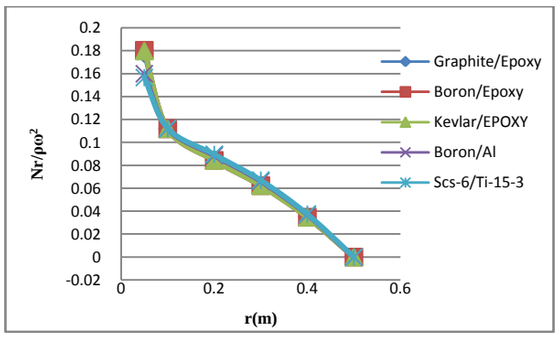

Fig. 10 Radial Stresses for Constraint Free Boundary Condition $[0/90/90/0]$

Radial stress distribution as a function of radius is graphically represented in figure 11 for fixed boundary condition; Fig shows Boron /Epoxy showing high radial stresses towards inner radius when compared to other composite materials and Kevlar/Epoxy showing minimum towards inner radius. At r = 0.1 the materials Kevlar/Epoxy, Scs-6/Ti-15-3, Boron/Al showing maximum stress values.

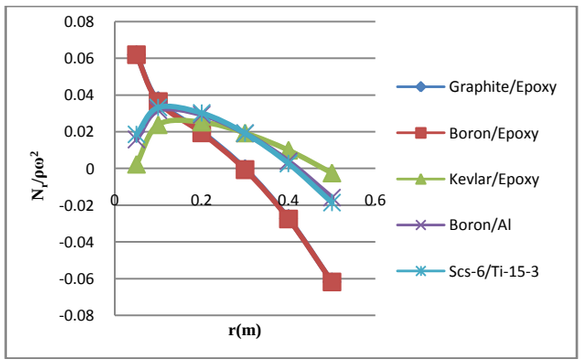

Fig. 11 Radial Stresses for Fixed Boundary Condition [0/90/90/0]

Figure 12 shows the radial displacements as a function of radial distance for constraint free boundary condition. Boron/Epoxy showing high Radial displacement at r = 0.3m at the outer radius Scs-6/Ti-15-3 is showing higher values. For Kevlar/Epoxy the displacement values are very small compared to remaining all other materials. Is larger than other composites and lowest displacement is displayed by graphite/epoxy composite.

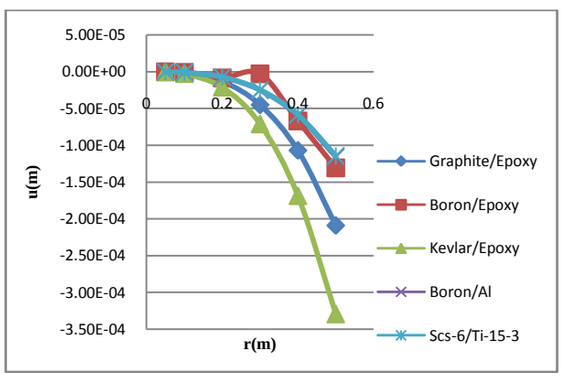

Fig. 12 Radial Displacements for Constraint Free Boundary Condition [0/90/90/0]

Graphical representations of radial displacements as a function of radius are represented in figure 13 for fixed boundary condition. Radial displacements vary from zero at inner radius to maximum at the midpoint and finally reaching zero at outer radius for all composites. The variation of displacements is maximum for Kevlar/Epoxy and lower for Graphite/Epoxy and Scs- 6/ Ti-15-3. The displacements are higher in constraint free boundary than in fixed boundary.

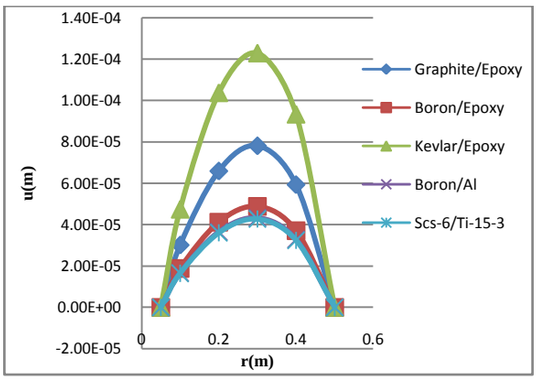

Fig. 13 Radial Displacements for Fixed Boundary Condition [0/90/90/0]

6. Conclusions

i. Effect of centrifugal forces on stresses and displacements have been studied for different composite laminated rotating discs when the stiffness ratio is equal to 1 and ply thickness equal to 0.25mm. Two boundary conditions are considered:
   a. The outer boundary is free of constraint
   b. The outer boundary is fixed.

ii. It is observed that Kevlar/Epoxy and Scs-6/Ti-15-3 composites are significant in terms of radial stresses. Kevlar/Epoxy shows higher values of stress and Scs-6/Ti-15-3 composite on the lower side.

iii. Cross ply laminated disc has higher values of stress than angle ply laminates with 45^0 fiber angle orientation.

iv. The radial displacements are larger for angle ply laminates than for cross ply laminates.

References

1. *Seirag A S and Surana K S (1970), "Optimum Design of Rotating Disks", Journal of Engineering for Industry, 1-10.*

2. *Murthy D N S and Sherbourne A N (1970), "Elastic Stresses in Anisotropic Disks of Variable Thickness" International Journal of Mechanical Science, Vol. 12, 627-640.*

3. *Reddy T Y and Srinath H (1974), "Eelastic Stresses in a Rotating Annular Disk of Variable Thickness and Density", Vol. 17, 397-402.*

4. *Chang C I (1975), "The Anisotropic Rotating Disks", International Journal of Mechanical Science, Vol. 17, 397-402.*

5. *Gurushankar G V (1975), "Thermal Stresses in a Rotating Non-Homogeneous Anisotropic Disk of Varying Thickness and Density", Journal of Strain Analysis, Vol. 10, 137-42.*

6. *Christensen R M and Wu E M (1977), "Optimal Design of Anisotropic (Fiber-Reinforced) Flywheel", Journal of Composite Materials, Vol. 11, 395-404.*

7. *Genta G and Gola M (1981), "The Stress Distribution in Orthotropic Rotating Disks", Journal of Applied Mechanics, Vol. 48, 559-620.*

8. *Bert C W (1975), "Centrifugal Stresses in Arbitrarily Laminated, Rectangular Anisotropic Circular Disks", Journal of Strain Analysis, Vol. 10, 84-92.*

9. *Mostaghel N and Tadjbakhsh I (1973), "Buckling of Rotating Rods and Plates", International Journal of Mechanical Science, Vol. 15, 429 -434.*

10. *Gamer U and Tresca's (1983), "Yield Condition and Rotating Disk", International Journal of Mechanical Transactions of ASME Vol. 50, 676-678.*

11. *Gamer U (1984), "Elastic-Plastic Deformation of the Rotating Solid Disk", Ingeniur ARCHIV Vol. 54, 345-354.*

12. *Gamer U (1984), "Elastic-Plastic Stress Distribution in the Rotating Annulus and in the Annulus Under External Pressure",, Zeitschnift for Angen Wandte Mathematik and Mechanik, Vol. 64, T126-T128.*

13. *Guven U (1992), "Elastic- Plastic Stresses in a Rotating Annular Disk of Variable Thickness and Variable Density", International Journal of Mechanical Science, Vol. 34, 133-138.*

14. *Sterner S C, Saigal S, Kistler W and Dietrich D E (1993), "A Unified Numerical Approach for the Analysis of Rotating Disks Including Turbine Rotors", International Journal of Solids and Structures, Vol. 31, 269-277.*

15. *Naki Tutuneu (1995), "Effect of Anisotropy on Stresses in Rotating Disks", International Journal of Mechanical Science, Vol. 37, 873-881.*

16. *Jen-San chen and Jhi-Lu Jhu (1996), "In-plane Response of a Rotating Annular Disk Under Fixed Concentrated Edge Loads", International Journal of Mechanical Science, Vol.38, 1285-1293.*

17. *Rajeev Jain Ramachandra K and Sinha K R Y (1998), "Rotating Anisotropic Disk of Uniform Strength", International Journal of Mechanical Science, Vol. 41, 639-648.*

18. *Singh S B and Ray S (2002), "Modeling the Anisotropy and Creep in Orthotropic AlSiC Composite Rotating Disc", Mechanics of Materials, Vol. 34.*

19. *Singh S B and Ray S (2003), "Newly Proposed Yield Criterion for Residual Stress and Steady State Creep in an Anisotropic Composite Rotating Disc", Journal of Materials Processing and Technology, Vol. 143.*

20. *Gupta V K (2004), "Steady State Creep and Material Parameters in a Rotating Disc of Al-SiCp Composite", European Journal of Mechanics A/Solids, Vol. 23.*

21. *Jahed H, Farshi B and Bidabadi J (2005), "Minimum Weight Design of Inhomogeneous Rotating Discs". International journal of Pressure Vessels and Piping.*

22. *Sayman O and Arman Y (2006), "Thermal Stresses in a Thermoplastic Composite Disc under a Steady State Temperature Distribution", Journal of Reinforced Plastics and Composites, Vol. 25, 1709–1722.*

23. *Çallıolu H (2007), "Thermal Stress Analysis of Curvilinear Orthotropic Rotating Discs", Journal of Hermoplasting Composite Materials.*

24. *Singh S B (2008), "One Parameter Model for Creep in a Whisker Reinforced Anisotropic Rotating Disc of Al-SiCw Composite", European Journal of Mechanics A/Solids.*

25. *Bayat M, Saleem M, Sahari B B, Hamouda A M S and Mahdi E (2009), "Mechanical and Thermal Stresses in a Functionally Graded Rotating Disc with Variable Thickness due to Racially Symmetry Loads".*

26. *Van Paepegem W and Degrieck J (2001), "Experimental Set-up for and Numerical Modeling of Bending Fatigue Experiments on Plain Woven Glass/Epoxy Composites", Vol. 51, 1–8.*